

# Molecular dynamic simulations of $\beta$ type medical titanium alloys with induced micro-structural damage under noncontinuous proton radiation: A nanoparticle model study

Y. Lei<sup>1</sup>, Y. Liu<sup>2</sup>, W. Zhang<sup>1\*</sup>, F. Chu<sup>3</sup>, T. Guo<sup>2</sup>

<sup>1</sup>Radiology Department, Beijing Chaoyang Hospital of Capital Medical University, Beijing, China

<sup>2</sup>Faculty of Civil Engineering and Mechanics, Kunming University of Science and Technology, Chenggong District, Kunming, Yunnan Province, China

<sup>3</sup>College of Aerospace and Civil Engineering, Harbin Engineering University, Harbin, Heilongjiang Province, China

## ABSTRACT

### ► Original article

#### \*Corresponding author:

Weiguo Zhang, M.D.

#### E-mail:

zhangweiguo0906@sina.com

Received: September 2024

Final revised: February 2024

Accepted: April 2024

Int. J. Radiat. Res., July 2025;  
23(3): 743-750

DOI: 10.61186/ijrr.23.3.32

**Keywords:** Radiology, molecular dynamic simulation, titanium, nanoparticles.

**Background:** Medical Titanium (Ti) alloys have been widely used in the fields of wound repair and orthopedic treatment because of their high strength, good resistance to physiological corrosion and excellent biomechanics properties. However, similar with other metal materials, Medical Ti alloys may also be damaged with potentially suffer from damages of various extent varying degrees under proton radiation condition and environment. **Materials and Methods:** As the Since traditional investigation methods are limited on time and space size to some extent, Molecular Dynamic (MD) simulations are generally applied to uncover the entire proton radiation process, and the simulated simulation models are concentrated on  $\beta$  type medical Ti alloys. **Results:** Firstly, when the proton struck with a constant velocity of 2000 Å/ps impact with Primary Knock-on Atom (PKA) at a constant velocity of 2,000 Å/ps, the kinetic energy of 24,451.7 eV will be transferred, and PKA will leave its original site and further transfer the kinetic energy, until reaching the equilibrium site, but accompanied by . This process also leave a plenty of significant micro-structure damages. Secondly, by adjusting the velocity of proton to be in the range of 1,500 Å/ps ~ 2,500 Å/ps, damage zone could be expanded by increasing the kinetic energy of proton. through adjusting the velocity of proton between 1500 and 2500 Å/ps, it seems that the addition of proton kinetic energy could enlarge the damage zone. However, the increase of increased Ti alloy matrix temperature did not have a great impact on the velocity of proton. could not show the same effect with proton velocity. Thirdly, the multi-proton effect on horizontal mode is more obvious pronounced than that on vertical mode. **Conclusions:** It is kinetic energy, but not rather than potential energy, that contributes to the formation of micro-structure in Ti alloys. The influence of temperature can be ignored in practical applications, In the practice environment, effects of temperature can be ignored, but the velocity and density of incident proton ought to be considered.

## INTRODUCTION

Due to the remarkably good remarkable performances on corrosion resistance, mechanical parameters and especially the excellent biocompatibility, biomedical applications (1) of Ti alloys have been increasingly present in biochemical applications (1) developed rapidly in decades in recent decades (2). According to the lattice type and parameters of Ti, there are three types of Ti alloys can be divided into three categories, namely, including  $\alpha$ -Ti,  $\beta$ -Ti and the hybrid of ( $\alpha$ + $\beta$ )-Ti (3), of which. It is said that  $\alpha$ -Ti is said to be consisted by composed of Hexagonal Close-Packed (HCP) structure, so its deformation is limited by the active slip systems (4). While, while  $\beta$ -Ti has show exhibits different strengthening mechanisms and mechanical properties with from  $\alpha$ -Ti (5). As for the In terms of

( $\alpha$ + $\beta$ )-Ti, the Ti-6Al-4V alloy is one of the most representative one that applied in for biomedical applications (6).

It is previously found that the Previous studies have shown that high elastic modulus of metal materials will cause Stress Shielding Effect (SSE) because of high elastic modulus, and low stress stimulation is not conducive to stimulating the self-healing function of human body and harmful to the healing of bone cracks (7). Therefore,  $\beta$  type -Ti alloy has received more and more attention in biomedicine applications.

The first generation includes pure Ti and the Ti-6Al-4V alloy. Ti-6Al-4V is characterized by has good corrosion resistance, low elastic modulus (110-130 GPa) and excellent strong plastic matching. Meanwhile, compositions of Al and V may be released in practical applications, which may increase the risk

of can be released in real applications and this may increase the risk of getting neurodegenerative diseases, such as the peripheral neuropathy, osteomalacia and Alzheimer's disease<sup>(8)</sup>.

Therefore, in the 1980s, Germany and Switzerland researchers replaced V with Fe and Nb, respectively, and developed the second generation of  $\alpha+\beta$  phase medical Ti alloy, which is represented by Ti-5Al-2.5Fe and Ti-6Al-7Nb<sup>(9, 10)</sup>. They have similar mechanical properties and better good bio-compatibility with Ti-6Al-4V, but the influence of Al element is not cannot be completely excluded<sup>(11)</sup>.

Furthermore, the developments of biomedical Ti alloys remains a global concern. still attracts extensive attention worldwide. Since the 1990s, countries around the world have successively carried out the research and development of low elastic modulus  $\beta$  type -Ti alloys that do not contain toxic elements such as Al and V, which is the third generation of medical Ti alloys. This study In the present study, selected the most representative Ti-12Mo-6Zr-2Fe<sup>(12)</sup>, Ti-35Nb-13Ta-4Mo<sup>(13)</sup> and Ti-24Nb-4Zr-7.9Sn<sup>(14)</sup> alloys, the most representative medical Ti alloys, were selected for following MD simulation.

With the increasing application of radiation therapy in cancer treatment<sup>(15)</sup> and other biomedicine fields<sup>(16-19)</sup>, medical metal implants have been threatened by radiations, like the increase of such as increased dislocations rate<sup>(20)</sup>. Therefore, it is necessary to explore the effects of radiation on Ti alloy materials, which has become a new research direction in many fields. So various effects of radiation on Ti alloy materials is necessary to become a new research direction in many fields. In recent years, it is reported has been reported that the formation of  $\beta$  phase can could enhance the solubility of hydrogen in Ti-Mo alloy, so the defects density in Ti-Mo alloy is lower than that of pure Ti, and the addition of Mo element helps to regulate the effect of radiation on is useful for the adjustment of radiation effect of Ti alloy<sup>(21)</sup>. Besides, in the low-energy ion implanting process, the addition of implantation in the low-energy ion implanting process also relates to the formation of vacancy defects in Ti<sup>(22)</sup>. Additionally, T. Ishida *et al.* believe that the presence of high density nano-precipitates may declared that the existence of nano precipitates with high density may enhance the radiation damage resistance of specific  $\beta$  type- Ti alloy<sup>(23)</sup>.

Currently, traditional radiation experiments have shown its limitations to some extent. Since metal specimen and characterization equipment may be damaged in the radiation testing environment, it is very difficult to control and monitor radiation process. As the radiation testing environment not only damages the metal specimen, but also the characterization equipment. On this occasion, the process control and monitoring of radiation is hard to

be accomplished. However was originally developed for atomic systems, and it is applicable for the radiation simulations. In 2017, Liu *et al.*<sup>(24)</sup> applied MD simulations to study the displacement cascade in gold nanowires and observed stacking faults when .the In which the formation of stacking faults could be observed when kinetic energy s of PKA is was higher than 5.0 keV. In 2024, He *et al.*<sup>(25)</sup> also investigated the Ti-6Al-4V alloys by MD simulations and made comparisons with pure Ti. Besides, Verkhovtsev *et al.*<sup>(26)</sup> reviewed the radiation Radiation-Driven Molecular Dynamics (IDMD) as a novel concept and simulation method. Despite Ti alloys, MD simulations are also applied for other microstructure damage issues<sup>(27, 28)</sup>.

Those previous reports Previous reports have shown the feasibility of MD simulations in the radiation of metals. In this study, the simulation models are The simulation models used in the present study are focused on the  $\beta$  type -Ti alloys, including Ti-12Mo-6Zr-2Fe, Ti-35Nb-13Ta-4Mo and Ti-24Nb-4Zr-7.9Sn. Then the micro-structure damage mechanism and affecting parameters are discussed. will be discussed below. Those The obtained results will help to enhance the understanding of micro-damage for Ti alloys in under radiation conditions. This study aims to provide a novel insight into the damages to medical Ti alloy damages, as well as then explore the application of MD simulations in noncontinuous proton radiation and its related damages on bio-alloys.

## MATERIALS AND METHODS

### Atomic potentials in MD

The Lennard-Jones (LJ) potential energy function applied in this study is a common mathematical model used to describe the interaction force between molecules<sup>(29, 30)</sup>. This constraint accompanies the calculation all the time. All LJ parameters applied in this study are listed in table 1 below table 1. The underlying theoretical framework of MD is Newton's law of motion served as the underlying theoretical framework of MD<sup>(31, 32)</sup>. In MD simulations, the The potential energy of each atom is was obtained from atomic charge, mass and coordinates during MD simulation. The coordination and movement of each atom were updated in each timestep In each timestep, coordination and movements of all atoms will be updated<sup>(33)</sup>. The performing of MD simulation was performed is based on LAMMPS<sup>(34, 35)</sup>, a classical MD software developed by American Sandia National Laboratories.

### Simulation models

In this study, the incident proton is was assumed to be accelerated vertically. Its velocity was a constant when When it is was close to the Ti alloy

surface, its velocity is a constant. As can be seen from figure 1 shows, the entire simulation contained involved a simulation box, proton and Ti alloy. The sizedimension of Ti alloy wason three dimensions are  $40 \times 40 \times 50 \text{ \AA}^3$ , and a proton is was placed above the Ti alloy surface, with a their vertical distance ofis  $20 \text{ \AA}$ . Then both proton and Ti alloy wereare placed in a  $100 \times 100 \times 100 \text{ \AA}^3$ . Other zones despite Except proton and Ti alloy, other regions were vacant are vacancy in thisduring MD simulation. There are totally threeA total of three types of medical Ti alloys were investigated in this study. As figure 1 shows, As shown in figure 1, these Ti alloy models are were Ti-12Mo-6Zr-2Fe, Ti-24Nb-4Zr-7.9Sn and Ti-35Nb-13Ta-4Mo (wt%). Among them, Ti-12Mo-6Zr-2Fe is discussed in Sections section 3.1 and 3.2 to demonstrate the mechanism of proton radiation, while Ti-24Nb-4Zr-7.9Sn and Ti-35Nb-13Ta-4Mo are discussed in sectionSection 3.3 to make further comparisons between different types of Ti alloys.

**Table 1.** Parameters for LJ potential in Ti alloys <sup>(36, 37)</sup>.

Number	Element	Epsilon (kcal/mol)	Sigms ( $\text{\AA}$ )
22	Ti	0.055	4.54
42	Mo	0.056	3.052
40	Zr	0.069	3.124
26	Fe	0.055	4.54
41	Nb	0.059	3.165
73	Ta	0.081	3.17
50	Sn	0.567	4.392
1	Proton	0.056	2.362

Despite the single proton model, more protons are were also modeled to studied explore other parameters of incident protons. As figure 2 shows, theseThese protons were placed muti-protons are placed vertically or horizontally, as shown in figure 2. These models in figurefigure 2 (a), (b), (c), (d) and (e) are were named as Model single, V4, V8, H4 and H5, respectively. Those mentioned comparisons on multi-protons arewere simulated for Ti-12Mo-6Zr-2Fe alloy matrix only. All simulations models in the study arewere rendered and visualized by OVITO program <sup>(38)</sup> program.

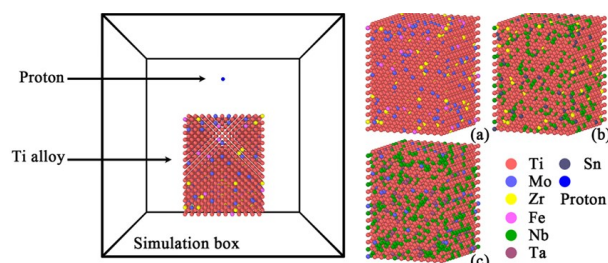


**Figure 1.** Proton and Ti alloy in the simulation box, (a): Ti-12Mo-6Zr-2Fe; (b): Ti-24Nb-4Zr-7.9Sn; (c): Ti-35Nb-13Ta-4Mo

### Performing Performance parameters

For all MD simulation models used in this study, a series of unique performing performance parameters are were applied to make further comparison between different models. In Among them, which the

initial velocity of proton is was fixed at  $2,000 \text{ \AA/ps}$ , and a microcanonical ensemble (NVE) iswas applied forto all atoms <sup>(39)</sup>. Initially, all atoms are were at  $300 \text{ K}$ , then thermostat iswas turned off. The timestep of MD simulations is was set as  $0.01 \text{ fs}$ , and each model iswas integrated for totally  $30,000$  steps in total.

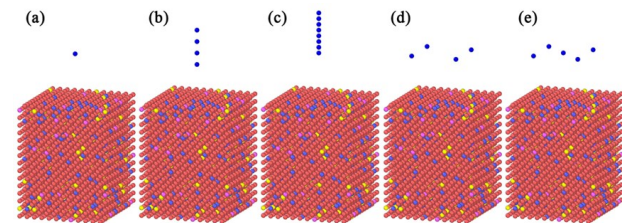


**Figure 2.** Simulations models with one (a), four (b, d), five (e) and eight (c) protons.

The only deviations on performing parameters are about proton velocity and matrix temperature, in order to discuss the change of proton radiation condition. Therefore, the velocity of proton is also to be was also respectively set as  $1500 \text{ \AA/ps}$  and  $2500 \text{ \AA/ps}$ . and matrix temperature as As for the temperature of matrix,  $500 \text{ K}$  and  $800 \text{ K}$  are also set respectively for the discussions onto clarify damage effects under the condition of same proton radiation condition.

## RESULTS

### The formation of induced micro-structural damage

It could be shown in the figure 3 thatIt can be seen from figure 3 that with the interatomic impact between incident proton and PKA, a series of cascade collision appearsoccurred. In  $0-6 \text{ fs}$ , proton keeps kept moving withat a constant velocity of  $2,000 \text{ \AA/ps}$ , andwithout affecting atoms in Ti alloy matrix are not affected. While However, at about  $12 \text{ fs}$ , the proton impactsaffected the surface atom, which is also called as known as the PKA. Then, a series of cascade collision appears emerged from  $12-30 \text{ fs}$ . While And at  $30 \text{ fs}$ , a plenty of atoms in Ti alloy displaced by around  $0-0.5 \text{ \AA}$ .

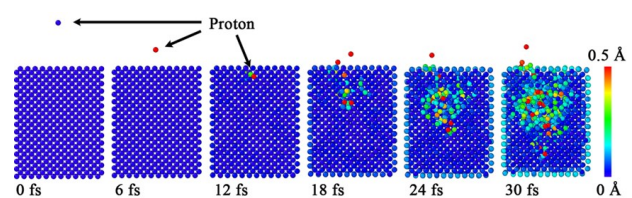


**Figure 3.** Entire The entire damage process of Ti-12Mo-6Zr-2Fe alloy (coloured by atomic displacements).

With the occurrence of the chain reaction on atomic movements in the styleform of cascade collision, there iswas no doubt that the micro-structure of the Ti-12Mo-6Zr-2Fe alloy is was damaged to somea certain extent. The majority of the phase of Ti-12Mo-6Zr-2Fe alloy, as a  $\beta$ -Ti alloy, was a body-centered cubic (BCC) latticeAs a  $\beta$  type titanium



alloy, the majority phase of Ti-12Mo-6Zr-2Fe alloy is in the style of Body Centered Cubic (BCC) lattice. At this moment, the microstructure of Ti alloy is was damaged by interatomic impact and kinetic energy transfer. In other words, the formation of induced micro-structural damage is damages were initiated started by the incident proton, and then enlarged by a chain of the chain reactions on atomic movements. In the entire cascade collision process, it seems that the interatomic transfer of energy is was a critical factor leading to the extension of for the extending of microstructure damages. For In terms of energy calculation energy computation induring MD simulations, the total energy of each atom, or even the entire system, could be divided into two sub items:, namely potential energy and kinetic energy. Therefore, the transfer of kinetic energy transfer is was the main factor that determines determining the severity the extent of microstructure damages.

In figure 4, the The lattice type of Ti-12Mo-6Zr-2Fe alloy is was identified by Ackland-Jones<sup>(40)</sup> algorithm, as shown in figure 4. It is shown that, It is obvious that the BBC type microstructure remained unchanged was not changed in 10 fs, and this is because the PKA is not impacted was not affected by the proton. Since about 12 fs, in figure 4, the content of BCC in Ti-12Mo-6Zr-2Fe alloy is declined with the appearance of cascade collision, as displayed in figure 4. While And at the same time, more and more an increasing number of atoms are were identified in the amorphous phase were identified.

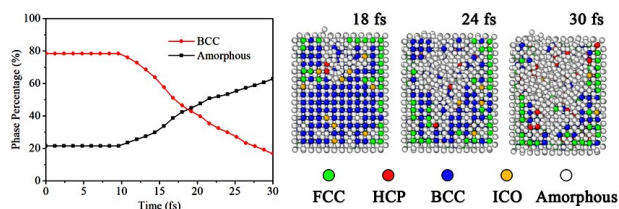


**Figure 4.** The change of micro-structure in 30 fs (by Ackland-Jones<sup>(40)</sup> analysis).

In figure 5, it seems that It can be seen from figure 5 that both potential and kinetic energies both contributes the climb of contributed to the increased total energy in this system. However, the item of kinetic could be seen as the “source” of micro-structure change, and the item of potential energy as the “result” to some extent.

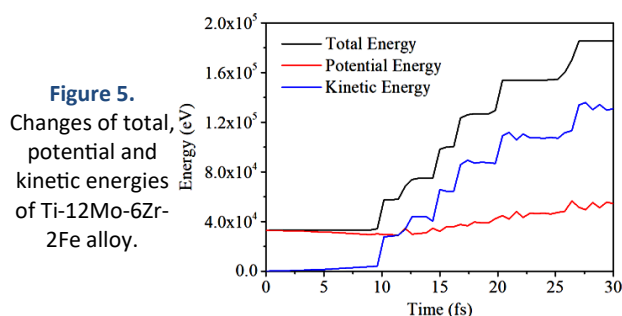
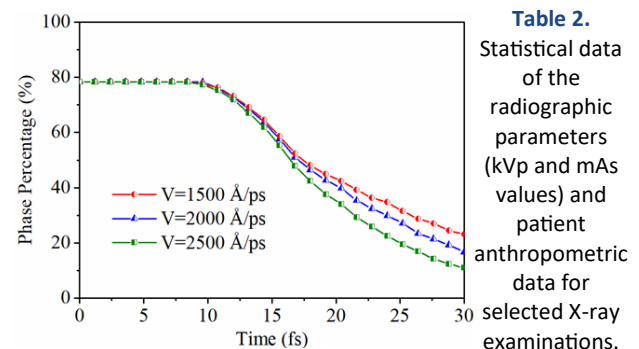


**Figure 5.** Changes of total, potential and kinetic energies of Ti-12Mo-6Zr-2Fe alloy.

### Effects of proton radiation parameters on damages

Figure 6 illustrates the change of BCC phase in  $\beta$  type- Ti alloy from 30 fs, in which the velocity of proton are were changed revised to be in the range of 1,500 Å/ps and  $\sim$  2,500 Å/ps. It seems that the There seemed to be insignificant differences among three models are not obvious in 0-10 fs, as in this process the proton is not impacted with did not have an impact on PKA or the impact is was not large enough to lead the damage of damage micro-structure. Then with the progress of cascade collision, differences on the decline of BCC phase become larger and larger were enlarged since 10 fs. While However, at 20-30 fs, it could be explicitly shown that the proton with high velocity or large kinetic energy will cause more micro-structure damages for the Ti alloy matrix at 20-30 fs.



Besides, it is also shown in figure as shown in figure 7 that the atom, atoms with high kinetic energy is were more likely to be concentrated on the “bottom” of damage zone. This is because the atoms after cascade collision were are prone to be equilibrated in a certain amorphous phase site after cascade collision. While However, the spread of cascade collision might continue to spread after kinetic energy transfer may continues further. The mechanism is not only on the energy between proton and PKA, but also on other neighbour atoms in the Ti alloy matrix. Initially, the kinetic energy of Ti alloy atoms at 300 K is was around 1.8-2.6 eV. While However, as shown in figure 7, a plenty of atoms are were displaced with when the kinetic energy of was nearly or over 100 eV. At the same moment (30 fs), it seems that the spread area of cascade collision spread further gets larger, especially on in the vertical direction, when the proton impacts affected the PKA at a with larger higher velocity.

Figure 8 demonstrates the decline of BBC phase in the Ti-12Mo-6Zr-2Fe alloy matrix while with at different temperatures. By statistics methods, it seems that the damage of micro-structure is was not as obvious as those caused by cause of proton acceleration. From beginning to the end ending (simulation stopped at 30 fs), the curves of BBC phase percentage are were almost the same, with minor deviations of about and deviation between curves are

little, about 2-3%.

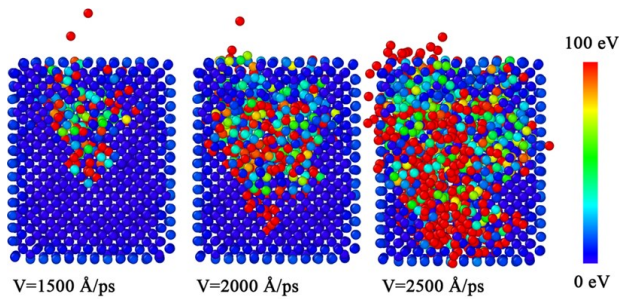


**Figure 7.** Slices of Ti alloys at 30 fs with different proton velocities (coloured by atomic kinetic energy).

Despite little difference in statistics, detailed comparisons could still be made by in situ observations of MD simulation result. Figure 9 shows the atomic potential energy distribution in Ti alloys at 30 fs. The increase of potential energy illustrates the decline in the distance decline or even nearly impacted between pairs of atoms. It could be observed in figure from figure 9 that the high potential energy regions are concentrated at the “bottom” of damage zone, which is where cascades collision spread.

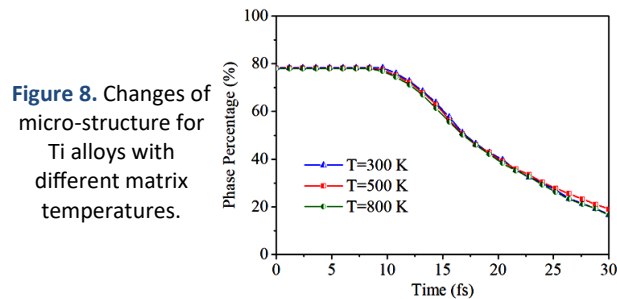


**Figure 8.** Changes of micro-structure for Ti alloys with different matrix temperatures.

Figure 10 illustrates the development of micro-structure damage. Comparing with the Model: Single, Model: V4 has little effects had a minor effect on the decline of BCC phase. Then if the vertical proton density is was introduced added tintoo the Model: V8, the BCC curve trends tended to be lower than before, but with limited deviation. but the extent of deviation is limited. Next, theThe horizontal models (Model: H4 and H5) explicitly acceleratesaccelerated the decline of BCC phase, as shown in figure 10. in figure 10.

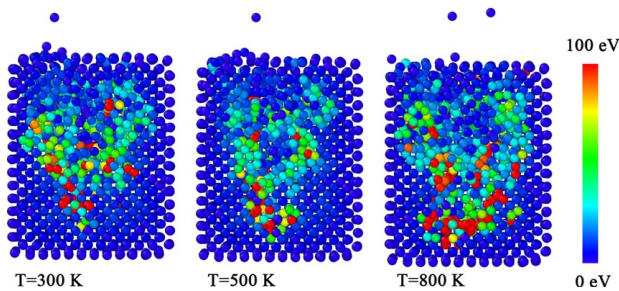


**Figure 9.** Slices of Ti alloys at 30 fs with different matrix temperatures at 30 fs (coloured by atomic potential energy).

Additionally, figure figure 11 is the top view of Models: Single, V4, V8, H4 and H5. It could be observed that The Models: Single, V4 and V8 are were

damaged at the same site. To some extent, increasing the proton density vertically can releasehelped to release more kinetic energy, but could not enlarge the area of incident effect. However, Models: H4, H5 increase increased the proton density horizontally. To some extent, it is a kind of multi-site incident mode, so the spread of impact effect was continued in a superimposed manneris overlaid.

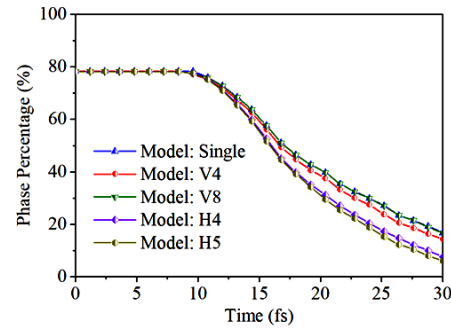


**Figure 10.** Changes of micro-structure for Ti alloys with different proton density.

### Comparisons between different $\beta$ type -Titanium alloys

Among all  $\beta$  type titanium-Ti alloys, Ti-12Mo-6Zr-2Fe, Ti-24Nb-4Zr-7.9Sn and Ti-35Nb-13Ta-4Mo are all developed for biomedical applications. They have different microstructure stability in the same proton radiation environmentWhen they are under the same proton radiation environment, the stability of micro-structure are various as well.

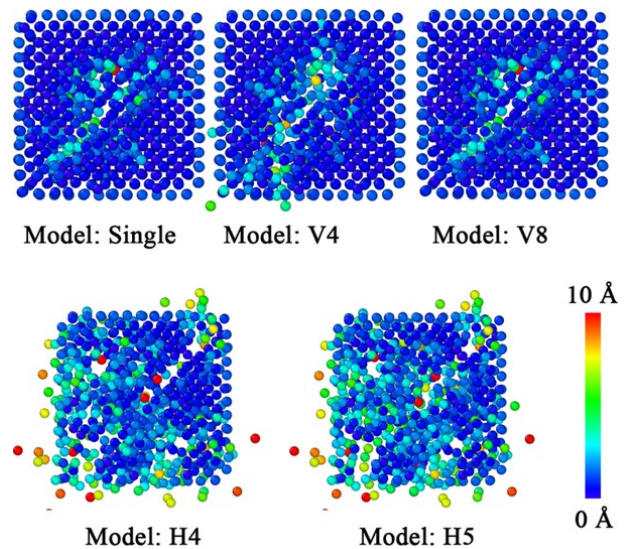


**Figure 11.** Slices of Ti alloys at 30 fs with different proton density (coloured by atomic displacements).

According to the curve of BCC phase decline in figure shown in figure 12 (a), it seems that the micro-structure damages of Ti-12Mo-6Zr-2Fe is a little lowerwas slightly less significant than that those of Ti-24Nb-4Zr-7.9Sn and Ti-35Nb-13Ta-4Mo before 25 fs. As because its lower the percentage of BCC phase in Ti-12Mo-6Zr-2Fe is higher than that of Ti-24Nb-4Zr-7.9Sn and Ti-35Nb-13Ta-4Mo. Besides, figure figure 12 (b) also demonstrates that atomic movement obtained by the kinetic energy for Ti-35Nb-13Ta-4Mo is explicitlywas explicitly better than that

obtained by the other models. To some extent, these differences between each Ti alloy are more likely to be caused by alloying atoms. Figure 13 shows the atomic displacements of each element in Ti-12Mo-6Zr-2Fe, Ti-24Nb-4Zr-7.9Sn and Ti-35Nb-13Ta-4Mo alloys.

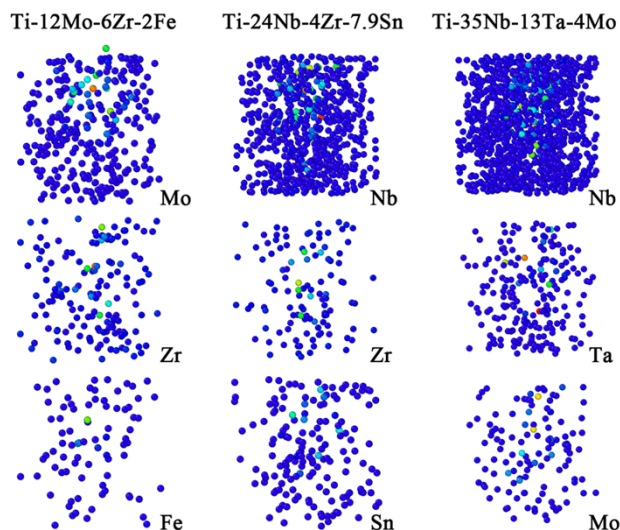


Figure 13. Atomic displacements of each element in three  $\beta$ -type Ti alloys.

## DISCUSSION

Due to the appearance of incident proton, severe damages are simulated to occur may form in Ti alloys. Although this phenomenon has been verified by high intensity proton beam tests<sup>(23)</sup>, the entire process and theory for the occurrence of damage is still weak. In this study, this aspect of damage occurrence was uncovered. Taking the Ti-12Mo-6Zr-2Fe alloy as the case example, in the radiation process, its kinetic energy was transferred from the proton with high velocity to the PKA at a high velocity in the radiation process, which is in good agreement with other studies<sup>(27)</sup>. Then, the PKA were moved with under the action of high kinetic energy (about 24,451.7 eV). This value is a little higher than that of Ti-6Al-4V, studied by He *et al.*<sup>(25)</sup>, so studies on different Ti alloys is necessary when reference energy values for PKA might change. An *et al.*<sup>(22)</sup> said that the implantation energy strongly determines the formation rate of vacancy type defects. In this study, the implantation energy has already been large enough to make move the PKA leave from its original lattice site. If the implantation energy here could lead to the chain reaction on atomic movements, then more and more atoms were affected and thus left their original lattice sites. Thus, it is deduced that there should be a critical boundary for implantation energy.

By comparing with reference<sup>(21, 28)</sup>, apart from the velocity of proton, matrix temperature is another factor that may affect the formation of damages in medical Ti alloys. According to the physical common

sense and reference<sup>(33)</sup>, if the temperature of Ti alloy matrix is high enough, those atoms in matrix will not be limited by in situ vibration, but leave their original sites in lattice. This so called as, known as the melting process. It is observed in this study, when the temperature of the Ti alloy matrix is in a high temperature, about 500-800 K, the *in situ* vibration is enlarged and the inhibition to the effect of the atomic impact is weakened. To some extent, Sun *et al.*<sup>(39)</sup> said that the laser induced ignition of Ti alloy is also based on this process.

Ishida *et al.*<sup>(23)</sup> applied the high intensity proton beam to study the radiation damage effect on titanium. The high intensity transferred in MD simulations could be the density of incident proton. Plenty of negative effects on the micro-structure damages of Ti alloys is found due to the variation of the proton radiation model in practical applications<sup>(20)</sup>, because in the practice environment, the proton radiation model are various. Additionally, It seems that the spread of cascade collision is related to the content of alloying elements. As the first major alloying elements, like Mo<sup>(21)</sup> and Nb<sup>(14)</sup>, contributes to the impact effect, so the atomic displacement of these atoms are higher than those of other elements.

However, due to the limited MD simulation capacity, there are still many limitations to be addressed in this study. For example, Verkhovtsev *et al.*<sup>(26)</sup> approved that MD simulations is successfully applied in irradiation. But quantitative analysis is still weak in many references. We also need to investigate more quantitative analysis methods. For example, deep statistical analysis methods have been applied in food<sup>(41)</sup>, bioscience<sup>(42, 43)</sup> and radiation related health researches<sup>(44, 45)</sup>. Finally, we also need to include more cases<sup>(1)</sup> to further improve the reliability of the research results.

## CONCLUSION

MD simulations are generally in this study to present the formation of micro-structure damage. Consequently, it seems that the transfer of kinetic energy, not potential energy, is the critical factor that determines the effect of cascade collision. Therefore, further accelerating the proton may enlarge the damage effect. However, the heating treatment between 300-500 K shows little effects on micro-structure effects. The horizontal addition of proton density can effectively enlarge the formation of amorphous phase.

## ACKNOWLEDGMENT

The authors team would like to express their appreciations to all the co-workers and their affiliations that supported and contributed to this investigation.



**Funding:** This work was supported by National Natural Science Foundation of China (NSFC) Project (Grant No: 52369017).

**Conflicts of interest:** The authors team declare that there is no conflict of interest in this study.

**Ethical consideration:** Not applicable.

**Authors' contributions:** Y.L.: Writing original manuscript draft; Y.L.: Data curation, investigation and formal analysis; W.Z.: Conceptualization and supervision; F.C.: Reviewing and investigation; T.G.: Project Management.

**Data Availability declaration:** The data are available from the corresponding authors on reasonable request.

## REFERENCES

- Rack HJ and Qazi JI (2006) Titanium alloys for biomedical applications. *Materials Science and Engineering: C*, **26**(8): 1269-1277.
- Sun R and Mi G (2023) Influence of alloying elements content on high temperature properties of Ti-V-Cr and Ti-Al-V series titanium alloys: A JMatPro program calculation study. *Journal of Physics: Conference Series*, **2639**: 012019.
- Yan M, Luo SD, Schaffer GB, Qian M (2012) TEM and XRD characterisation of commercially pure  $\alpha$ -Ti made by powder metallurgy and casting. *Materials Letters*, **72**: 64-67.
- Thota MK, Kapoor R, Basak CB, Mukherjee AB, Chakravartty JK (2015). High temperature deformation of  $\alpha$ -Ti. *Materials Science and Engineering: A*, **624**: 213-219.
- Kao YL, Tu GC, Huang CA, Liu TT (2005) A study on the hardness variation of  $\alpha$ - and  $\beta$ -pure titanium with different grain sizes. *Materials Science and Engineering: A*, **398**(1-2): 93-98.
- Huang Q, Liu X, Yang X, Zhang R, Shen Z, Feng Q (2015) Specific heat treatment of selective laser melted Ti-6Al-4V for biomedical applications. *Frontiers of Materials Science*, **9**(4): 373-381.
- Banerjee D and Williams JC (2013). Perspectives on titanium science and technology. *Acta Materialia*, **61**: 844-879.
- Mohammed MT, Khan ZA, Manivasagam G, Siddiquee AN (2015) Influence of thermomechanical processing on biomechanical compatibility and electrochemical behavior of new near beta alloy, Ti-20.6Nb-13.6Zr-0.5 V. *International Journal of Nanomedicine*, **10**: 223-235.
- Semlitsch M (1987) Titanium alloys for hip joint replacements. *Clinical Materials*, **2**(1): 1-13.
- Shen X, Shukla P, Nath S, Lawrence J (2017) Improvement in mechanical properties of titanium alloy (Ti-6Al-7Nb) subject to multiple laser shock peening. *Surface and Coatings Technology*, **327**: 101-109.
- Geetha M, Singh AK, Asokamani R, Gogia AK (2009) Ti based biomaterials, the ultimate choice for orthopaedic implants - A review. *Progress in Materials Science*, **54**(3): 397-425.
- Yang X and Hutchinson CR (2016) Corrosion-wear of  $\beta$ -Ti alloy TMZF (Ti-12Mo-6Zr-2Fe) in simulated body fluid. *Acta Biomaterialia*, **42**: 429-439.
- Cai D, Chen D, Zhang G, Yu Y (2019) Research progress of medical titanium alloys. *China Medical Device Information*, **25**(9): 43-45.
- Hao YL, Li SJ, Sun SY, Zheng CY, Yang R (2007) Elastic deformation behaviour of Ti-24Nb-4Zr-7.9Sn for biomedical applications. *Acta Biomaterialia*, **3**(2): 277-286.
- Chen Z, Dominello MM, Joiner MC, Burmeister JW (2023) Proton versus photon radiation therapy: A clinical review. *Frontiers in Oncology*, **13**: 1133909.
- Huynh TYH, Truong HNT, Trinh HL, Nguyen VT, Le CH (2024) Improvement of the accuracy of radioactivity analysis using gamma spectroscopy by reducing the Compton continuum of 40K gamma spectrum. *International Journal of Radiation Research*, **22** (3): 565-572.
- Song S, Lee YS, Kim W, Choi M, Kim S, Bae H, et al. (2024) Anti-inflammatory effects of low-dose rate ionizing radiation on cell lines derived from osteoarthritis patients. *International Journal of Radiation Research*, **22**(3): 585-593.
- Yavas MC, Kilitci A, Çelik E, Yegin K, Sirav B, Varol S (2024) Rat brain and testicular tissue effects of radiofrequency radiation exposure: Histopathological, DNA damage of brain and qRT-PCR analysis. *International Journal of Radiation Research*, **22**(3): 529-536.
- Luo Y, Peng C, Deng Q, Song H, Zhai S, Zhou Q (2024) Application of ultrasonography and 99mTc-MIBI scintigraphy in the diagnosis and localization of hyperparathyroidism. *International Journal of Radiation Research*, **22**(1): 97-101.
- Yang L, Chen Y, Miller J, Weber WJ, Bei H, Zhang Y (2024) Nanoindentation study on early-stage radiation damage in single-phase concentrated solid solution alloys. *Materials Science & Engineering A*, **908**: 146746.
- Shi Y, Wang Q, Yang Q, Song Z, Wan M, Ma R, et al. (2023) Effect of Mo alloying on vacancy-defect evolution and irradiation damage in titanium alloy. *Journal of Alloys and Compounds*, **968**: 172130.
- An X, Zhang H, Zhu T, Wang Q, Zhang P, Song Y, et al. (2022) Exploration of vacancy defect formation and evolution in low-energy ion implanted pure titanium. *International Journal of Hydrogen Energy*, **47**(13): 8467-8479.
- Ishida T, Wakai E, Hagiwara M, Makimura S, Tada M, Asner DM, et al. (2018). Study of the radiation damage effect on Titanium metastable beta alloy by high intensity proton beam. *Nuclear Materials and Energy*, **15**: 169-174.
- Liu W, Chen P, Qiu R, Khan M, Liu J, Hou M, Duan J (2017) Nuclear instruments and methods in physics research section B: Beam interactions with materials and atoms. *Nuclear Instruments and Methods in Physics Research Section B: Beam Interactions with Materials and Atoms*, **405**: 22-30.
- He T, Li X, Qi Y, Zhao M, Feng M (2024) Molecular dynamics simulation of primary irradiation damage in Ti-6Al-4V alloys. *Nuclear Engineering and Technology*, **56**(4): 1480-1489.
- Verkhovtsev AV, Solov'yov IA, Solov'yov AV (2021) Irradiation-driven molecular dynamics: a review. *The European Physical Journal D*, **75**: 213.
- Cui J, Hou Q, Li M, Fu B (2024) Effect of applied strain on radiation damage in CoCrFeNi concentrated solid solution alloys: Insights from molecular dynamics simulations. *Nuclear Inst and Methods in Physics Research, B*, **552**: 165378.
- Wei G, Byggmästar J, Cui J, Nordlund K, Ren J, Djurabekova F (2024) Revealing the critical role of vanadium in radiation damage of tungsten-based alloys. *Acta Materialia*, **274**: 119991.
- Wang Z, Guo K, Wang C, Zhang D, Tian W, Qiu S, Su G (2022) Molecular dynamics study of liquid sodium film evaporation and condensation by Lennard-Jones potential. *Nuclear Engineering and Technology*, **54**(8): 3117-3129.
- Wang Y, Xu J, Wang Q (2023) Molecular dynamics simulation and nonlinear analysis of density fluctuations in Lennard-Jones fluid system near the critical point. *Chinese Journal of Physics*, **84**: 132-151.
- Tang Y, Fu Z, Raos G, Ma F, Zhao P, Hou Y (2024) Molecular dynamics simulation of adhesion at the asphalt-aggregate interface: A review. *Surfaces and Interfaces*, **44**: 103706.
- Li X, Liu Y-j, Nian B-b, Cao X-y, Tan C-p, Liu Y-f, Xu Y-j (2022) Molecular dynamics revealed the effect of epoxy group on triglyceride digestion. *Food Chemistry*, **373**: 131285.
- Sun R, Mi G, Huang X, Sui N (2024) Molecular dynamic simulations of Ti-6Al and Fe-12Cr alloys for their heat transfer and oxygen transport behaviors. *Modern Physics Letters B*, **38**: 2350263.
- Thompson AP, Aktulga HM, Berger R, Bolintineanu DS, Brown WM, Crozier PS, et al. (2022) LAMMPS - a flexible simulation tool for particle-based materials modeling at the atomic, meso, and continuum scales. *Computer Physics Communications*, **271**: 108171.
- Plimpton S (1995) Fast parallel algorithms for short-range molecular dynamics. *Journal of Computational Physics*, **117**(1): 1-19.
- Rappe AK, Casewit CJ, Colwell KS, III WAG, Skiff WM (1992) UFF, a full periodic table force field for molecular mechanics and molecular dynamics simulations. *Journal of the American Chemical Society*, **114**(25): 10024-10035.
- Mayo SL, Olafson BD, Goddard WA (1990) DREIDING: a generic force field for molecular simulations. *Journal of Physical Chemistry*, **94**(26): 8897-8909.
- Stukowski A (2009) Visualization and analysis of atomistic simulation data with OVITO—the open visualization tool. *Modelling and Simulation in Materials Science and Engineering*, **18**(1): 015012.

39. Sun R and Mi G (2024) Investigations on the surface temperature field of Ti-6Al and Ti-48Al alloy under continuous laser ablation. *Rare Metal Materials and Engineering*, **53**(9): 2405-2412.
40. Ackland G and Jones AP (2006) Applications of local crystal structure measures in experiment and simulation. *Physical Review B*, **73**(5): 054104.
41. Xue Li, Yanjun Liu, Yong-jiang Xu, Yuanfa Liu (2024) System-wide coordination and communication of lipid metabolism atlas revealed cytotoxicity of epoxy triglyceride in deep-frying oil. *Food Bioscience*, **59**: 104193.
42. Xiujuan Lin, Fangfang Liu, Zihan Ma, Xue Li, Yang Li (2025) Investigating the impact of beeswax addition and diacylglycerol profiles on bigel properties and application in bread: Insights on intermolecular interaction mechanisms. *Food Hydrocolloids*, **160**: 110838.
43. Yang Cheng, Xiujuan Lin, Bolin Xu, Xue Li, Yang Li (2024) Oleogel formation based on natural insoluble soybean fiber using capillary force: A novel strategy and application. *International Journal of Biological Macromolecules*, **282**: 137361.
44. Chi YM and Chang CC (2024) Axillary lymph nodes's response to pneumococcal polysaccharide vaccination on FDG-PET/CT examination: Two case reports. *International Journal of Radiation Research*, **22**(4): 1095-1097.
45. Xia TF, Zhang ZJ, Guo X (2024). Effects of DNA methyltransferase 2 (DNMT2) on gastric cancer cells proliferation and migration via regulation of structural maintenance of chromosomes 3 (SMC3). *International Journal of Radiation Research*, **22**(4): 897-902.